Local Induction of Acetylcholine Receptor Clustering in Myotube Cultures Using Microfluidic Application of Agrin

Anna Tourovskaia, T. Fettah Kosar, and Albert Folch
Department of Bioengineering, University of Washington, Seattle, Washington 98195-2255

ABSTRACT During neuromuscular synaptogenesis, the exchange of spatially localized signals between nerve and muscle initiates the coordinated focal accumulation of the acetylcholine (ACh) release machinery and the ACh receptors (AChRs). One of the key first steps is the release of the proteoglycan agrin focalized at the axon tip, which induces the clustering of AChRs on the postsynaptic membrane at the neuromuscular junction. The lack of a suitable method for focal application of agrin in myotube cultures has limited the majority of in vitro studies to the application of agrin baths. We used a microfluidic device and surface microengineering to focally stimulate muscle cells with agrin at a small portion of their membrane and at a time and position chosen by the user. The device is used to verify the hypothesis that focal application of agrin to the muscle cell membrane induces local aggregation of AChRs in differentiated C2C12 myotubes.

INTRODUCTION

The adult neuromuscular synapse is characterized by a high density of acetylcholine receptors (AChRs) on the postsynaptic muscle cell membrane (1,2). Despite decades of research, the process by which AChRs aggregate (cluster) at the site of contact between the nerve and the muscle cell is still not fully elucidated. A key signal for AChR clustering is the release of agrin by the axon terminal as the growing axon arrives at the muscle cell membrane during development (2–4). However, the exact role of neural agrin is still not clear since AChR clusters have been found in the embryo in the absence of innervation (5–8) as well as in pure myotube cultures (9–12), which indicates that signals other than neural agrin can trigger the mechanism that leads to AChR cluster formation. The relative role of these agrin- and nerve-independent clusters as compared to the agrin-induced clusters is, for lack of quantitative methods, unknown. As synapse formation plays a critical role in the correct development of the organism, experimental manipulation of agrin in vivo has been difficult. Therefore, the effects of agrin have been most often studied in vitro—usually in cell cultures of myotubes. In these experiments neural agrin is seen to induce aggregation of AChR as well as other molecules associated with the postsynaptic apparatus (3,13). Most of these studies have relied on bathing the entire surface of the myotube with agrin-containing solution (13), which induces the formation of AChRs clusters at multiple random locations. When myotubes are exposed to agrin only locally—using agrin released by nerve cells or expressed by CHO cells (1,14–16) or adsorbed agrin micropatterns (17,18)—AChR clusters form preferentially on the agrin-stimulated sites. Although these methods provide useful models for studying synaptogenic molecules, such focal presentation of immobilized agrin on randomly organized myotubes (1,14–18) suffers from an inherent uncertainty in the presented concentrations and lack of control over the time, duration, and/or location of the agrin stimulus.

Here we attempt to mimic the presence of the neuron in the first stages of the formation of a neuromuscular synapse by inducing localized AChR clustering using laminar flow (19) in a microfluidic device to deliver agrin at a precise location, time, and dose onto C2C12 myotubes. We set the delivery to occur at a physiologically relevant time after C2C12 myoblasts have fused into myotubes displaying normal agrin-independent AChR clusters. The myotubes are spatially organized on microengineered substrates so as to be parallel with each other and to have approximately the same length and width. After the center portion of the myotubes is exposed to agrin, AChR clusters form only at the agrin-stimulated areas. Thus, our results corroborate the prevailing hypothesis that focalized stimulation of the muscle cell membrane with agrin induces AChR clustering at the stimulated site and provides a useful tool for further studies on AChR clustering. The experimental setup is amenable to quantitative design of the spatiotemporal microenvironment of the cells and produces rich statistics by stimulating many myotubes simultaneously.

MATERIALS AND METHODS

Device fabrication and operation

The microfluidic device used in this study consists of a set of elastomeric channels assembled on top of a glass slide as previously described (20). Briefly, it was formed of two orthogonally connected fluidic networks, one consisting of three inlet channels converging into a 2-cm-long, 1500-μm-wide, and 250-μm-high main channel and the other one consisting of 16 51-μm-wide and 40-μm-high perfusion channels that intersect with the main channel (Fig. 1). The devices were made by replica molding in poly(dimethylsiloxane) (PDMS) (21). The PDMS replicas were cured overnight at 65°C and

Submitted September 20, 2005, and accepted for publication December 8, 2005.

Address reprint requests to Albert Folch, E-mail: afolch@u.washington.edu.

0006-3495/06/03/2192/07 $2.00

doi: 10.1529/biophysj.105.074864

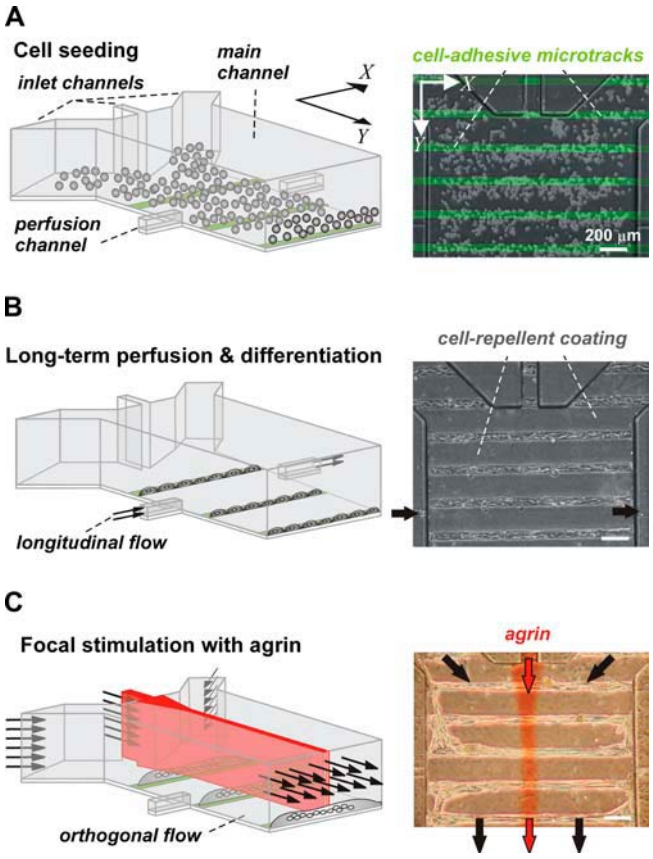

FIGURE 1 Microfluidic cultures of micropatterned C2C12 myotubes. (*A–C*) Three-dimensional schematics of the experimental design (*left column*) and the corresponding phase-contrast images of the device (*right column*). (*A*) C2C12 myoblasts are introduced into the device through the inlet channels and allowed to attach to 30–40 μm-wide microtracks of adhesive proteins (Polylysine/Matrigel, in *green*); (*B*) continuous long-term cell perfusion in the *x* direction (longitudinal flow) is started (*black arrows*); (*C*) after myotubes are formed (~1.5 weeks), the longitudinal flow is blocked and orthogonal flow is started to stimulate the cells with a heterogeneous stream containing agrin at the center (*red arrows*) and no agrin on either side (*black arrows*). The agrin-containing stream appears red because a red dye was added to the agrin solution for visualization purposes.

autoclaved. The master molds were fabricated by two-layer photolithography of the photoresist SU-8 2035 (for Layer I) and SU-8 2100 (for Layer II) (MicroChem, Newton, MA) according to the manufacturer's datasheets. The three converging inlet channels and the perfusion channels were defined in Layer I; the main channel was defined in Layer II. This two-layer architecture effectively adds high flow resistance, which serves the purpose of minimizing the sensitivity of flow rates to fluctuations in driving pressure while allowing for a relatively large chamber (the main channel) for the cells (20). After the cells mature within the microfluidic channels (placed inside a traditional cell culture incubator), flow in the *x* direction is blocked and flow in the *y* direction is started using the three inlet channels (Fig. 1 *C*). Flow in the devices was driven by gravity using constant flow syringes (CFS) (Warner Instruments, Hamden, CT) that contained gas- and thermally equilibrated cell culture medium as described (20). The stability and the width of the agrin stream were monitored by addition of the food-coloring dye Allura (2.5 μg/mL) (Sigma-Aldrich, St. Louis, MO) to the agrin-carrying stream (we have not observed any obvious toxicity effects derived from the exposure of the myotubes to the food dye). The supplemental movie (phase-contrast) demonstrates the high stability of the flows in the device over a 2-h period with images acquired every 2 min. The Allura stream appears as a dark band in phase-contrast images and as a large negative peak in the intensity line scans (100 pixels wide) taken across the channel (see Supplemental Fig. 4 *A*). The position of the Allura peak is defined as the peak's centroid in the intensity line scans. The width of the stream is taken as the full width at the half-height of the Allura peak in the intensity line scan (see Supplemental Fig. 4 *C*).

Surface modification for directed myotube growth

The glass substrate is chemically micropatterned to restrict the areas available for cell attachment and myotube formation (20,22). Micropatterns of cell-adhesive microtracks alternating with a cell-repellent coating were prepared using oxygen plasma etching and elastomeric masks as reported previously (20,22). Briefly, glass wafers were grafted with interpenetrating polymer networks (IPNs) of poly(ethyleneglycol) and poly(acrylamide). Next, PDMS microchannels (30–40 μm wide and 65 μm tall) were used as masks for etching IPNs to expose bare glass, to which cell attachment-promoting molecules (poly-D-lysine and growth factor-reduced Matrigel) were subsequently adsorbed. The microchannels were then removed. The micropatterned substrate and the microfluidic PDMS device were exposed to O_2 plasma (Branson/IPC 2000 barrel etcher, 150 W, 0.75 Torr, 40 s) and bonded together (23) so that protein micropatterns were aligned orthogonal to the main channel. To protect the protein pattern from being degraded by the O_2 plasma, the pattern was covered with a slab of PDMS that covers the protein pattern and seals around it.

Cell culture and reagents

The C2C12 subclone (24) of the mouse myogenic cell line C2 (25) was purchased from American Type Cell Culture (ATCC, Manassas, VA). All culture media and reagents were obtained from Life Technologies (Bethesda, MA) unless otherwise specified. Matrigel matrix was purchased from BD Biosciences (Bedford, MA). C2C12 cells were maintained as myoblasts in Dulbecco's modified Eagle's medium (DMEM) supplemented with 20% fetal bovine serum (FBS, HyClone, Logan, UT) and 1% penicillin-streptomycin-fungizone in 10% CO_2 incubator at 37°C. Cells were enzymatically removed from the culture flasks at subconfluence with 0.25% trypsin and 1 mM EDTA in Hanks' Balanced Salt Solution, resuspended in DMEM containing 20% serum, counted in a hemocytometer, injected into the microfluidic devices at ~2,000,000 cells/mL, and allowed to attach and spread on the Matrigel-coated microtracks for 15–30 min before continuous perfusion was established. Myoblast fusion into myotubes was promoted at confluency by low-serum differentiating medium (DM) (26) consisting of 2% horse serum (ATCC) and 1% penicillin-streptomycin-fungizone in DMEM. Typically within 4 days after switching the medium, myoblasts started fusing into myotubes, often spanning the entire width (in the *x* direction) of the channel. C2C12 cells were allowed to mature for ~9–10 days after switching to DM.

Agrin-induced AChR cluster induction and visualization of AChR clusters and agrin

Agrin (C-terminal fragment, C-$Ag_{3,4,8}$, molecular weight (MW) ~90 kDa) was purchased from R&D Systems (Minneapolis, MN). Myotubes were stimulated with saturating concentration of agrin (~10 nM) (27). The cells were either immersed in agrin solution in a Petri dish (agrin bath) or stimulated with a microfluidic stream containing agrin. For focal stimulation, the agrin stream was confined by two no-agrin streams under nonturbulent (laminar) flow conditions. For nonfocal stimulation, the agrin stream occupied the whole width of the main channel, exposing the whole length of the myotube to agrin (agrin flooding). Agrin stimulation lasted either for 18 h or 1 h, after which agrin was withdrawn (agrin bath experiments) or agrin flow stopped (microfluidic experiments). Finally, cells were

washed and incubated in agrin-free medium for 6 h (28). Next, the cells were labeled live with Alexa Fluor 488 and/or Alexa Fluor 594 conjugates of α-bungarotoxin (BTX, 500 ng/ml, 45 min) (Molecular Probes, Eugene, OR), which binds with high specificity to AChRs (29). Excess toxin was washed off; cells were fixed in 4% paraformaldehyde in phosphate buffered saline for 15 min at 37°C and imaged with an epifluorescence microscope. For anti-agrin immunostaining, a monoclonal mouse antibody (Agr 247, ab12364, Abcam, Cambridge, MA) was used (2 μg/ml). If needed, the real width of the agrin stream during focal stimulation may be inferred from the width of the red dye stream (see above) as follows. For a spherical molecule, the diffusion coefficient D is rather insensitive to changes in MW, $D \sim (MW)^{-1/3}$, and the mean diffusive path x is not very sensitive to changes in D, $x \sim D^{-1/2}$ (30). Hence we may scale the D of the agrin fragment ($MW_{agr} = 90{,}000$ Da), D_{agr}, from that of albumin ($MW_{alb} = 67{,}000$ Da, measured $D_{alb} = 6 \times 10^{-7}$ cm^2/s (31)), $D_{agr} \approx 5.4 \times 10^{-7}$ cm^2/s, and the D of red Allura ($MW_{Allu} = 496$ Da), D_{Allu}, from that of a typical molecule of $MW = 300$–500 Da (32), $D_{Allu} \approx 10^{-7}$ cm^2/s. Therefore, the mean diffusive path $x_{agr} \approx (D_{agr}/D_{Allu})^{-1/2} \times x_{Allu} \approx 0.4 \times x_{Allu}$, i.e., the diffusion profile of the agrin stream, is expected to be approximately on the order of 2.5 times narrower than that of Allura.

Imaging and quantification of AChR-clustering activity

Fluorescence and phase-contrast images were acquired on an inverted microscope (Eclipse TE2000-U, Nikon, Tokyo, Japan) with a charge-coupled device camera (ORCA-ER or ORCA-HR, Hamamatsu Photonics, Hamamatsu City, Japan) using commercial imaging software (MetaMorph, Universal Imaging, Downingtown, PA). Fluorescence images were captured in gray-scale (12-bit) and stored as 16-bit TIFF files. To assess the spatial distribution of AChR clusters, we applied a fine grid (10-pixel increment) to stitched images of myotubes (with the grid lines running orthogonal to the myotube long axis) and recorded the incidence of AChR cluster within the grid columns for each myotube. For a given myotube, columns containing at least a portion of one AChR cluster were assigned a value of 1, otherwise columns were assigned a value of 0. We then built a map of these 0s and 1s for each microtrack (*solid rectangular boxes* in Fig. 3, *A* and *B*; values of 1 are represented in *black* and values of 0 are represented in *white*). To obtain a quantitative measure of localization/spread of AChR clustering, for each microtrack we calculated the mean of the distances of all 1s to the left microchannel wall (termed ''center of mass'' of the AChRs (AChR-CM)) and the width of the region that encompasses 90% of the 1s around the AChR-CM (termed ''spread''). All routines were written in MATLAB (The MathWorks, Natick, MA).

RESULTS AND DISCUSSION

Differentiation of C2C12 myoblasts in microfluidic micropatterned cultures

Shown in Fig. 1 are schematic (*left column*) and representative (*right column*) pictures over the course of a typical experiment. The design of the microfluidic device allows for perfusion in two orthogonal directions x and y, parallel and perpendicular to the myotubes, respectively. A large channel enclosing the cells (main channel) intersects a set of shallow perfusion channels (Fig. 1 *A*). The three inlets of the main channel feed the flow in the y direction (orthogonal flow) and are used to seed C2C12 myoblasts at the beginning of the experiment (Fig. 1 *A*) as well as to generate heterogeneous laminar-flow streams perpendicular to the cells in the last phase of the experiment (Fig. 1 *C*). The cells attach to and align along the adhesive microtracks of poly-D-lysine/Matrigel surrounded by protein-repellent matrix (Fig. 1 *B*; see Materials and Methods). C2C12 cells are myogenic, i.e., they are capable of fusion into long multinucleated myotubes and expression of muscle-specific proteins. This differentiation process is enhanced by low serum-containing differentiating medium (DM), which inhibits myoblast proliferation (26). In our microfluidic cultures, after perfusing the cells with DM in the x direction (parallel flow, see Fig. 1 *B*) through the perfusion channels over a period of $\sim$1 week, C2C12 cells fuse to form myotubes in the x direction-oriented microtracks (Fig. 1 *C*; often two or more parallel myotubes form on the same microtrack). The cells were kept in a conventional humidified incubator under constant perfusion to avoid hyperosmolarity and acidification (common concerns in cell cultures confined to small environments (33,34)) during the week-long process of muscle cell fusion (20). To minimize shear stress on the cells from constant flow, the cells were perfused through 16 high-flow resistance channels orthogonal to the main channel, i.e., parallel to the long axis of the myotubes (longitudinal flow, see Fig. 1 *B* and Materials and Methods). No obvious change in the growth rates and cellular morphology was observed compared to the traditional agrin bath control cultures (i.e., nonmicropatterned and nonmicrofluidic, with cells cultured on glass or on tissue culture polystyrene coated with Matrigel) that were maintained in parallel with the microfluidic cultures. Estimated shear stresses on the cells due to either parallel or orthogonal flow ($\sim 1.3 \times 10^{-3}$ N/m^2 and $\sim 7.0 \times 10^{-3}$ N/m^2, respectively) were $\sim$3 orders of magnitude lower than the shear stresses known to compromise surface attachment of adherent cells (0.5–10.0 N/m^2) (35) or to affect cell viability, phenotype, metabolism, and/or protein expression (36,37).

Local induction of AChR clustering

Here we demonstrate a microfluidic approach to test the hypothesis that the focal stimulation of a small area of the myotube membrane with agrin entices the cell to recruit AChRs to that area. As shown in Fig. 2, we have used three experimental schemes that differ in the solutions introduced in the inlet channels (0 = no agrin, 1 = agrin): A) $\{000\}$: plain DM in all three inlet channels or no-agrin control (Fig. 2 *A*), B) $\{111\}$: agrin-containing medium in all three inlet channels or agrin-flooding control (Fig. 2 *B*), and C) $\{010\}$: agrin in the center channel only or focal agrin (Fig. 2 *C*). In both the $\{111\}$ and $\{010\}$ schemes, a food-coloring dye was added to the agrin streams for flow visualization (Fig. 1 *C*). Because the center inlet channel was designed with higher flow resistance than the side inlet channels, the agrin stream occupied only a $\sim$100–150 μm-wide portion at the center of the main channel (equal to $\sim$7%–10% of the width of the main channel). The position and width of the stream varied less than a few microns per hour (for flow stability measure-

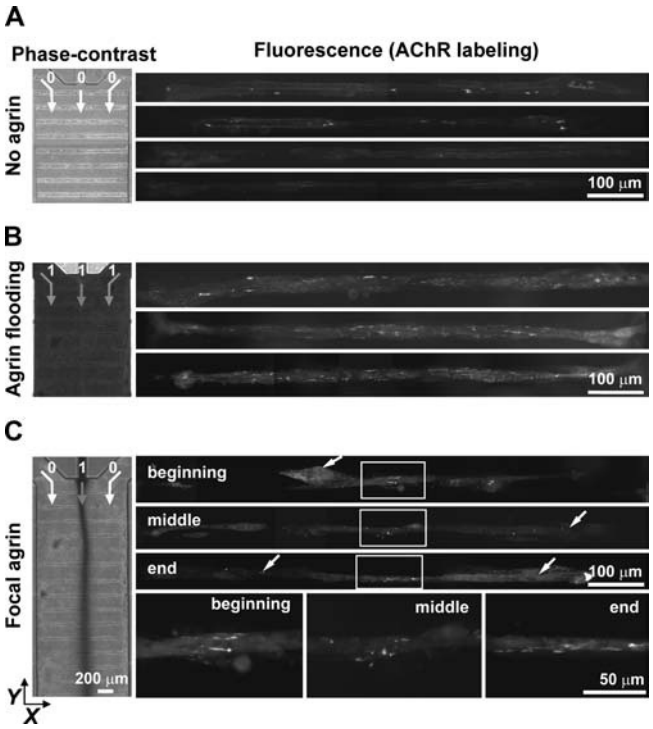

FIGURE 2 Focal exposure of central regions of C2C12 myotubes to agrin induces localized AChR clustering. (*A–C*) AChR aggregation response of myotubes to three different microfluidic stimulation schemes, (*A*) {000} (no-agrin control), (*B*) {111} (agrin flooding or homogeneous stream of agrin), and (*C*) {010} (focal agrin), where 0 and 1 indicate the absence and presence of agrin, respectively, in the three inlet channels that feed the main channel. The left-column images are phase-contrast micrographs taken during perfusion in the *y* direction (*arrows* denote the flow direction); the agrin-containing streams appear darker because a food-coloring dye was added to the agrin solutions for visualization purposes. The right-column images are fluorescence micrographs of AChR cluster staining (fluorescently conjugated α-BTX) corresponding to each scheme. White arrows point to the microclusters (see text).

ments, see Supplemental movie and Supplemental Fig. 4) and could, in principle, be controlled by varying the relative hydrostatic pressures and/or flow resistances of the three inlet channels. For simplicity, in the work presented here the agrin stream was always positioned at the center of the main channel; downstream deviations from the exact center were also stable in time and were attributable to the irregular cell-based topographies (e.g., Fig. 2 *C left image*). (The orientation of the myotubes perpendicular to the flow direction prevented the chaotic mixing that is typical of microchannels with surface features (38).) Shown in Fig. 2 are the AChR labeling results (*right column*) corresponding to the three schemes (depicted in the *left column*). The no-agrin control ({000} scheme) showed no AChR-aggregating effect (Fig. 2 *A*). On the other hand, the agrin-flooding control ({111} scheme, Fig. 2 *B*) induced the formation of numerous AChR clusters throughout the entire surface of myotubes, similar to nonmicrofluidic agrin-bath control cultures (see Supplemental Fig. 5). In the {010} scheme, myotubes responded to this stimulation by organizing AChRs into discrete clusters localized to the area where the agrin stream contacted the myotubes, as observed by AChR labeling (Fig. 2 *C*). Anti-agrin immunostaining (Supplemental Fig. 6) did not reveal agrin on the Matrigel microtracks themselves or on the surface of the myotubes, possibly because the recombinant carboxy-terminal agrin fragment (C-$Ag_{3,4,8}$) that was used for the flow experiments lacked the N-terminal domains responsible for interaction with the extracellular matrix (39,40). Therefore, the amount of agrin that remained associated with the myotubes can be considered negligible, so it should be possible to quantitatively correlate the spatial distribution of AChR clusters with the three-dimensional concentration profile of agrin surrounding the myotube (e.g., using confocal microscopy and a fluorescent tracer; efforts are underway).

To produce quantitative measures of AChR cluster distribution, for each experiment we constructed binary representations (0 = no clusters and 1 = AChR cluster(s)) of all the combined AChR-staining images from the whole device corresponding to myotubes that had been focally stimulated (Fig. 3 *A*) or flood stimulated (Fig. 3 *B*) with 10 nM agrin solution for 1 h (at 6 h of total experimental time). Microtracks with no myotubes or with out-of-focus clusters, which constituted only a small part of the collected data, were discarded from the analysis. Each of the microtrack areas filled with myotube(s) are schematically represented in Fig. 3, *A* and *B*, as long horizontal rectangular boxes (*solid borders*), with the vertical position of each box indicating the real relative position of the microtrack within the main channel (*y* axis). Black color indicates presence of AChR clusters in the corresponding portion of the myotube. The data show a gradual increase of the AChR clustering area toward downstream, likely due to the broadening of the diffusion profile of the agrin stream. Fig. 3 *C* shows the two cumulative graphs (arithmetic sums of 1s and 0s along the *y* axis for a given *x* axis position) corresponding to all the myotubes in Fig. 3, *A* and *B* (focal agrin and agrin bath in *black* and *gray*, respectively). Taken together, the data represented in Fig. 3, *A–C*, clearly demonstrate that 1) after agrin flooding, AChR cluster localization does not occur; and 2) after focal agrin application, the vast majority of AChR clusters localize around the centerline of the microchannel, with considerable heterogeneity in cluster distribution. To characterize the spatial distribution, for each microtrack we calculated its AChR center of mass (AChR-CM, average distance between AChRs and the left microchannel wall) and the spread of AChR cluster-containing areas (defined as the length of a segment containing 90% of all the clusters around the AChR-CM in a given microtrack). As an example, the AChR-CMs are indicated as gray marks in Fig. 3 *A*. The histogram in Fig. 3 *D* quantitatively summarizes the distribution of AChR clusters for a larger number of myotubes from two different focal agrin experiments ($n = 41$) and a control experiment ($n = 13$). The histogram of the AChR spread values correspond-

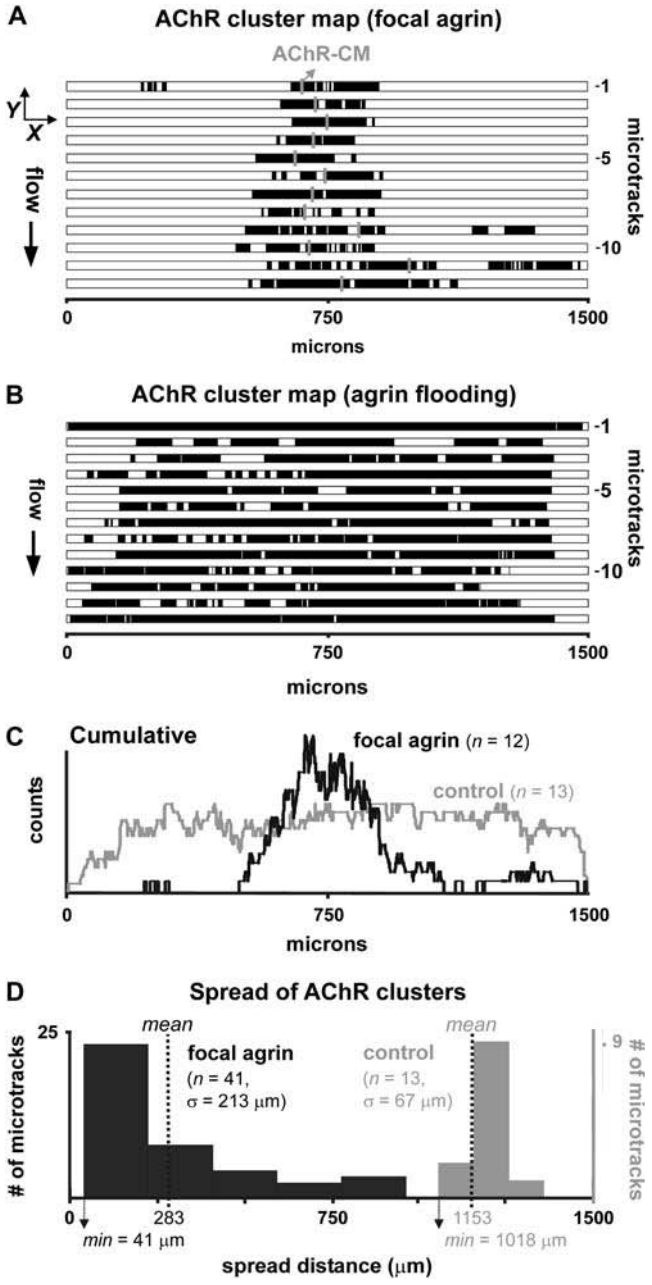

FIGURE 3 Spatial distribution of AChR clusters induced by focal agrin. (*A*, *B*) Binary maps of AChR clusters (*black areas*) for representative focal agrin (*A*) and control (*B*) experiments (1 h exposure to 10 nM agrin at 6 h total experimental time); each rectangular box represents one microtrack. The maps were produced from high-resolution micrographs of fluorescently labeled myotubes (such as those in Fig. 2) as described in the text. The *x* axis represents AChR cluster position relative to the left microchannel wall for all analyzed microtracks (with microtrack number in the *y* axis increasing toward downstream). In each microtrack, a gray vertical line indicates the center of mass of all AChRs (average distance between AChRs and the left microchannel wall) in that microtrack. (*C*) Plot of the cumulative sum of all binary cluster counts in (*A*) (*black*) and (*B*) (*gray*). (*D*) Spread of AChR clustering (spread = length of microtrack containing 90% of the clusters centered around the AChR center of mass) for focal agrin (*black*) and agrin flooding (*gray*) experiments. Black dotted vertical lines indicate the mean spread for both data sets.

ing to focal agrin ($n = 41$) delivery experiments (*black bins* in Fig. 3 *D*) shows that the majority of AChR clusters are localized within a short range (mean = 283 μm, min. = 41 μm, SD = 213 μm) around the AChR-CM. In contrast, the AChR spread histogram corresponding to agrin flooding (*gray bins* in Fig. 3 *D*) shows, as expected, that most of the cluster-containing areas are spread over distances approximating 90% of the width of the microchannel (mean = 1153 μm, min. = 1018 μm, SD = 67 μm).

We have occasionally observed that AChR cluster localization happens also on short, off-center myotubes that do not span the whole length of their microtrack (data not shown), indicating that the myotube center is not inherently privileged during the clustering process. Some AChR clusters (<6%) were seen outside of the stimulated area. They were either spontaneous clusters on short myotubes that did not intersect with the area of stimulation or small punctate clusters on stimulated myotubes (*white arrowheads* in Fig. 2 *C*) that might be the remnants of preexisting clusters. The presence of these outliers is in agreement with previous observations that agrin-independent AChR clusters also form in the embryo in the absence of innervation (5–8) as well as in pure myotube cultures using specific substrates (9–12) (see Fig. 2 *A* and Supplementary Figs. 5, *A*, *C*, and *E*, and 6 *F* for examples), which indicates that signals other than neural agrin can trigger the mechanism that leads to AChR cluster formation. Previous studies have demonstrated that agrin-independent clusters in random myotube cultures dissolve and reform in smaller sizes at random locations when exposed to agrin baths (41). Investigation of other explanations for the presence of AChR clusters away from the center of the channel, such as changes in shape or retraction of myotubes during the experiment, will require time-lapse imaging and is underway. Presently, the relative role of these agrin- and nerve-independent clusters as compared to the agrin-induced clusters is unknown.

CONCLUSIONS

To study the AChR clustering action of the synaptogenic molecule agrin, we have developed a microfluidic device that delivers a soluble stimulus to micropatterned myotubes with subcellular resolution. In essence, our microfluidic device represents an attempt to mimic the presence of the neuron in the first stages of the formation of a neuromuscular synapse. Even though flow is absent in the synaptic contact, our approach allows for mimicking local presentation of synaptogenic molecules and at the same time provides control over other parameters (location, duration, start, and end time points) of stimulation that previously could not be controlled simultaneously. Our data show that focal microfluidic application of agrin triggers local AChR clustering in C2C12 myotubes. A 1-h-long focal stimulation with agrin is sufficient to induce localized AChR clustering. The geometrical arrangement of the myotubes and their confinement to the precise locations

of a cell culture surface also allow for easy identification and high-throughput monitoring of single myotubes over time, making a culture readily amenable for quantitative analysis. The method offers a great control over the magnitude and spatiotemporal characteristics of the stimulus: it can be started at and applied for a specified time, easily removed, and, in principle, relocated and/or applied at separate different locations simultaneously, opening the way for studies of competitive stimuli and for more quantitative studies on AChR clustering dynamics when combined with live imaging.

SUPPLEMENTARY MATERIAL

An online supplement to this article can be found by visiting BJ Online at http://www.biophysj.org.

We are grateful to Drs. Marv Adams, Stanley Froehner, and Lisa Horowitz for insightful comments and to Mark Fauver for the peak tracking analysis program.

This work was funded by the National Institute of Biomedical Imaging and Bioengineering under grant No. R01-EB001474. A.T. acknowledges a fellowship from the Center for Nanotechnology at the University of Washington.

REFERENCES

1. Frank, E., and G. D. Fischbach. 1979. Early events in neuromuscular junction formation in vitro: induction of acetylcholine receptor clusters in the postsynaptic membrane and morphology of newly formed synapses. *J. Cell Biol.* 83:143–158.
2. Sanes, J. R., and J. W. Lichtman. 2001. Induction, assembly, maturation and maintenance of a postsynaptic apparatus. *Nat. Rev. Neurosci.* 2:791–805.
3. McMahan, U. J. 1990. The agrin hypothesis. *Cold Spring Harb. Symp. Quant. Biol.* 55:407–418.
4. McMahan, U. J., S. E. Horton, M. J. Werle, L. S. Honig, S. Kroger, M. A. Ruegg, and G. Escher. 1992. Agrin isoforms and their role in synaptogenesis. *Curr. Opin. Cell Biol.* 4:869–874.
5. Peng, H. B., and Y. Nakajima. 1978. Membrane particle aggregates in innervated and noninnervated cultures of Xenopus embryonic muscle cells. *Proc. Natl. Acad. Sci. USA.* 75:500–504.
6. Harris, A. J. 1981. Embryonic growth and innervation of rat skeletal muscles. III. Neural regulation of junctional and extra-junctional acetylcholine receptor clusters. *Philos. Trans. R. Soc. Lond. B Biol. Sci.* 293:287–314.
7. Lin, W., R. W. Burgess, B. Dominguez, S. L. Pfaff, J. R. Sanes, and K. F. Lee. 2001. Distinct roles of nerve and muscle in postsynaptic differentiation of the neuromuscular synapse. *Nature.* 410:1057–1064.
8. Yang, X., S. Arber, C. William, L. Li, Y. Tanabe, T. M. Jessell, C. Birchmeier, and S. J. Burden. 2001. Patterning of muscle acetylcholine receptor gene expression in the absence of motor innervation. *Neuron.* 30:399–410.
9. Fischbach, G. D., and S. A. Cohen. 1973. The distribution of acetylcholine sensitivity over uninnervated and innervated muscle fibers grown in cell culture. *Dev. Biol.* 31:147–162.
10. Sytkowski, A. J., Z. Vogel, and M. W. Nirenberg. 1973. Development of acetylcholine receptor clusters on cultured muscle cells. *Proc. Natl. Acad. Sci. USA.* 70:270–274.
11. Bekoff, A., and W. J. Betz. 1976. Acetylcholine hot spots: development on myotubes cultured from aneural limb buds. *Science.* 193: 915–917.
12. Kummer, T. T., T. Misgeld, J. W. Lichtman, and J. R. Sanes. 2004. Nerve-independent formation of a topologically complex postsynaptic apparatus. *J. Cell Biol.* 164:1077–1087.
13. Meier, T., and B. G. Wallace. 1998. Formation of the neuromuscular junction: molecules and mechanisms. *Bioessays.* 20:819–829.
14. Anderson, M. J., and M. W. Cohen. 1977. Nerve-induced and spontaneous redistribution of acetylcholine receptors on cultured muscle cells. *J. Physiol.* 268:757–773.
15. Sharp, A. A., and J. H. Caldwell. 1996. Aggregation of sodium channels induced by a postnatally upregulated isoform of agrin. *J. Neurosci.* 16:6775–6783.
16. Bromann, P. A., H. Zhou, and J. R. Sanes. 2004. Kinase- and rapsyn-independent activities of the muscle-specific kinase (MuSK). *Neurosci. Lett.* 125:417–426.
17. Jones, G., A. Herczeg, M. A. Ruegg, M. Lichtsteiner, S. Kroger, and H. R. Brenner. 1996. Substrate-bound agrin induces expression of acetylcholine receptor epsilon-subunit gene in cultured mammalian muscle cells. *Proc. Natl. Acad. Sci. USA.* 93:5985–5990.
18. Cornish, T., D. W. Branch, B. C. Wheeler, and J. T. Campanelli. 2002. Microcontact printing: a versatile technique for the study of synaptogenic molecules. *Mol. Cell. Neurosci.* 20:140–153.
19. Takayama, S., E. Ostuni, P. LeDuc, K. Naruse, D. E. Ingber, and G. M. Whitesides. 2001. Subcellular positioning of small molecules. *Nature.* 411:1016.
20. Tourovskaia, A., X. Figueroa-Masot, and A. Folch. 2005. Differentiation-on-a-chip: a microfluidic platform for long-term cell culture studies. *Lab Chip.* 5:14–19.
21. Xia, Y., and G. M. Whitesides. 1998. Soft lithography. *Angew. Chem. Int. Ed. Engl.* 37:550–575.
22. Tourovskaia, A., T. Barber, B. Wickes, D. Hirdes, B. Grin, D. Castner, K. E. Healy, and A. Folch. 2003. Micropatterns of chemisorbed cell adhesion-repellent films using oxygen plasma etching and elastomeric masks. *Langmuir.* 19:4754–4764.
23. McDonald, J. C., D. C. Duffy, J. R. Anderson, D. T. Chiu, H. K. Wu, O. J. A. Schueller, and G. M. Whitesides. 2000. Fabrication of microfluidic systems in poly(dimethylsiloxane). *Electrophoresis.* 21: 27–40.
24. Blau, H. M., G. K. Pavlath, E. C. Hardeman, C. P. Chiu, L. Silberstein, S. G. Webster, S. C. Miller, and C. Webster. 1985. Plasticity of the differentiated state. *Science.* 230:758–766.
25. Yaffe, D., and O. Saxel. 1977. Serial passaging and differentiation of myogenic cells isolated from dystrophic mouse muscle. *Nature.* 270: 725–727.
26. Linkhart, T. A., C. H. Clegg, and S. D. Hauschka. 1981. Myogenic differentiation in permanent clonal mouse myoblast cell lines: regulation by macromolecular growth factors in the culture medium. *Dev. Biol.* 86:19–30.
27. Ferns, M., M. Deiner, and Z. Hall. 1996. Agrin-induced acetylcholine receptor clustering in mammalian muscle requires tyrosine phosphorylation. *J. Cell Biol.* 132:937–944.
28. Mittaud, P., A. A. Camilleri, R. Willmann, S. Erb-Vogtli, S. J. Burden, and C. Fuhrer. 2004. A single pulse of agrin triggers a pathway that acts to cluster acetylcholine receptors. *Mol. Cell. Biol.* 24:7841–7854.
29. Lee, C. Y. 1972. Chemistry and pharmacology of polypeptide toxins in snake venoms. *Annu. Rev. Pharmacol.* 12:265–286.
30. Tanford, C. 1961. Physical Chemistry of Macromolecules. Wiley, New York.
31. Placidi, M., and S. Cannistraro. 1998. A dynamic light scattering study on mutual diffusion coefficient of BSA in concentrated aqueous solutions. *Europhys. Lett.* 43:476–481.
32. Goodhill, G. J. 1998. Mathematical guidance for axons. *Trends Neurosci.* 21:226–231.
33. Potter, S. M., and T. B. DeMarse. 2001. A new approach to neural cell culture for long-term studies. *J. Neurosci. Methods.* 110: 17–24.

34. Walker, G. M., M. S. Ozers, and D. J. Beebe. 2002. Insect cell culture in microfluidic channels. *Biomed. Microdevices.* 4:161–166.

35. Aunins, J. G., and H. J. Henzler. 1993. Aeration in Cell Culture Bioreactors. H. J. Rehm and G. Reed, editors. Wiley-VCH, Weinheim, Germany.

36. Nerem, R. M., R. W. Alexander, D. C. Chappell, R. M. Medford, S. E. Varner, and W. R. Taylor. 1998. The study of the influence of flow on vascular endothelial biology. *Am. J. Med. Sci.* 316:169–175.

37. Keane, J. T., D. Ryan, and P. P. Gray. 2003. Effect of shear stress on expression of a recombinant protein by Chinese hamster ovary cells. *Biotechnol. Bioeng.* 81:211–220.

38. Stroock, A. D., S. K. Dertinger, G. M. Whitesides, and A. Ajdari. 2002. Patterning flows using grooved surfaces. *Anal. Chem.* 74:5306–5312.

39. Denzer, A. J., M. Gesemann, B. Schumacher, and M. A. Ruegg. 1995. An amino-terminal extension is required for the secretion of chick agrin and its binding to extracellular matrix. *J. Cell Biol.* 131:1547–1560.

40. Denzer, A. J., R. Brandenberger, M. Gesemann, M. Chiquet, and M. A. Ruegg. 1997. Agrin binds to the nerve-muscle basal lamina via laminin. *J. Cell Biol.* 137:671–683.

41. Hoch, W. 1999. Formation of the neuromuscular junction. Agrin and its unusual receptors. *Eur. J. Biochem.* 265:1–10.